

LETTERS

Structural insight into the autoinhibition mechanism of AMP-activated protein kinase

Lei Chen^{1*}, Zhi-Hao Jiao^{1*}, Li-Sha Zheng^{2*}, Yuan-Yuan Zhang¹, Shu-Tao Xie¹, Zhi-Xin Wang^{1,2} & Jia-Wei Wu¹

The AMP-activated protein kinase (AMPK) is characterized by its ability to bind to AMP, which enables it to adjust enzymatic activity by sensing the cellular energy status and maintain the balance between ATP production and consumption in eukaryotic cells^{1,2}. It also has important roles in the regulation of cell growth and proliferation, and in the establishment and maintenance of cell polarity³. These important functions have rendered AMPK an important drug target for obesity, type 2 diabetes and cancer treatments⁴. However, the regulatory mechanism of AMPK activity by AMP binding remains unsolved. Here we report the crystal structures of an unphosphorylated fragment of the AMPK α -subunit (KD-AID) from *Schizosaccharomyces pombe* that contains both the catalytic kinase domain and an autoinhibitory domain (AID), and of a phosphorylated kinase domain from *Saccharomyces cerevisiae* (Snf1-pKD). The AID binds, from the 'backside', to the hinge region of its kinase domain, forming contacts with both amino-terminal and carboxy-terminal lobes. Structural analyses indicate that AID binding might constrain the mobility of helix α C, hence resulting in an autoinhibited KD-AID with much lower kinase activity than that of the kinase domain alone. AMP activates AMPK both allosterically and by inhibiting dephosphorylation^{5,6}. Further *in vitro* kinetic studies demonstrate that disruption of the KD-AID interface reverses the autoinhibition and these AMPK heterotrimeric mutants no longer respond to the change in AMP concentration. The structural and biochemical data have shown the primary mechanism of AMPK autoinhibition and suggest a conformational switch model for AMPK activation by AMP.

AMPKs are highly conserved heterotrimeric enzymes found in most eukaryotic species. The catalytic α -subunit contains a conventional Ser/Thr kinase domain, followed by an autoinhibitory sequence and a C-terminal segment for interacting with the β -subunit^{7,8} (Supplementary Fig. 1). The activity of AMPK is tightly regulated by upstream kinases through the phosphorylation of a conserved threonine (Thr 172 in rat) within the activation segment⁹. Furthermore, 5'-AMP that binds to the regulatory γ -subunit activates AMPK by eliciting allosteric changes and inhibiting pThr 172 dephosphorylation^{5,6,10}. The scaffold β -subunit bridges α - and γ -subunits by means of its C-terminal sequence, and contains a central non-catalytic glycogen-binding domain that may sense the status of cellular energy reserved in the form of glycogen^{11,12}. In addition to AMP, the thienopyridone A-769662 was reported to directly activate AMPK by an unexpected mechanism involving the glycogen-binding domain of the β 1-subunit, highlighting a regulatory role of the β -subunit in modulating AMPK activity¹³⁻¹⁶. Recently, the core structures of the $\alpha\beta\gamma$ heterotrimers from yeast and mammals, containing the whole γ -subunit but only the C-terminal interacting segments of the α - and β -subunits, have been independently

determined¹⁷⁻¹⁹. Because the critical kinase domain and autoinhibitory sequence were not included, many outstanding questions concerning the regulatory mechanism of AMPK activity remain, such as how the catalytic kinase domain is regulated by the autoinhibitory sequence and how AMP binding to the γ -subunit can ultimately enhance the kinase activity in the α -subunit.

We generated and purified the kinase domains and KD-AID fragments from rat and yeast AMPKs, and all proteins could be readily phosphorylated and activated by CaMKK β ¹⁵ (Supplementary Fig. 2). Like mammalian AMPK, the yeast KD-AID fragments were inactive in their unphosphorylated state, and exhibited low basal kinase activities when phosphorylated at the Thr residues (Thr 189 in *S. pombe* and Thr 210 in *S. cerevisiae*; Fig. 1a-c). The differences between the enzymatic activities of yeast kinase domains and those of KD-AID fragments were found to be around tenfold, comparable to the 17-fold increase of the rat kinase domain to its KD-AID⁷. These data demonstrate that the autoinhibitory property is evolutionarily conserved.

To determine the molecular and structural basis for the autoinhibition by the AID and the activation by upstream kinases, we solved a 2.8-Å structure of the unphosphorylated KD-AID fragment from *S. pombe* (Fig. 1d), and a 2.9-Å structure of the phosphorylated kinase domain from *S. cerevisiae* (Snf1-pKD) (Fig. 1e and Supplementary Fig. 3). Both kinase domains have the same canonical Ser/Thr protein kinase fold as those from *S. cerevisiae* Snf1 (Protein Data Bank (PDB) accession codes 3FAM and 2FH9)^{20,21} and human AMPK- α 2 (also known as PRKAA2; PDB accession codes 2H6D and 2YZA). The N-terminal lobe consists of a five-stranded antiparallel β -sheet and two α -helices, including the prominent helix α C, whereas the C-terminal lobe is dominated by α -helices. Snf1-pKD displays a 'closed' conformation, although the phosphorylated Thr 210 is invisible, whereas the unphosphorylated kinase domain of *S. pombe* KD-AID adopts an 'open' inactive conformation readily superimposed to Snf1-KD²² (Fig. 1f). The AID adopts a compact conformation consisting of three α -helices (α 1- α 3), and binds to the backside of the kinase domain through a new mechanism (see later).

Both structures comprise two molecules within an asymmetric unit that form head-to-tail dimers involving the activation segments and helices α G. Notably, the well-ordered activation segment of *S. pombe* KD-AID is jammed into its active site, and the critical catalytic residues make several intra- and intermolecular contacts (Supplementary Fig. 4). Such a dimeric interaction is expected to inhibit its kinase activity. To determine the biological significance of crystal packing interfaces of dimeric kinase domains²³, we first characterized the oligomeric state of AMPK fragments in solution (Supplementary Fig. 5). Unlike the kinase domain or the KD-AID fragment from *S. cerevisiae* that showed phosphorylation-dependent dimer-monomer switch, both unphosphorylated and phosphorylated *S. pombe* KD-AID were eluted as monomers. Similar results were obtained with the *S. pombe*

¹MOE Key Laboratory of Bioinformatics, Department of Biological Sciences and Biotechnology, Tsinghua University, Beijing 100084, China. ²Institute of Biophysics and Graduate University, Chinese Academy of Sciences, Beijing 100101, China.

*These authors contributed equally to this work.

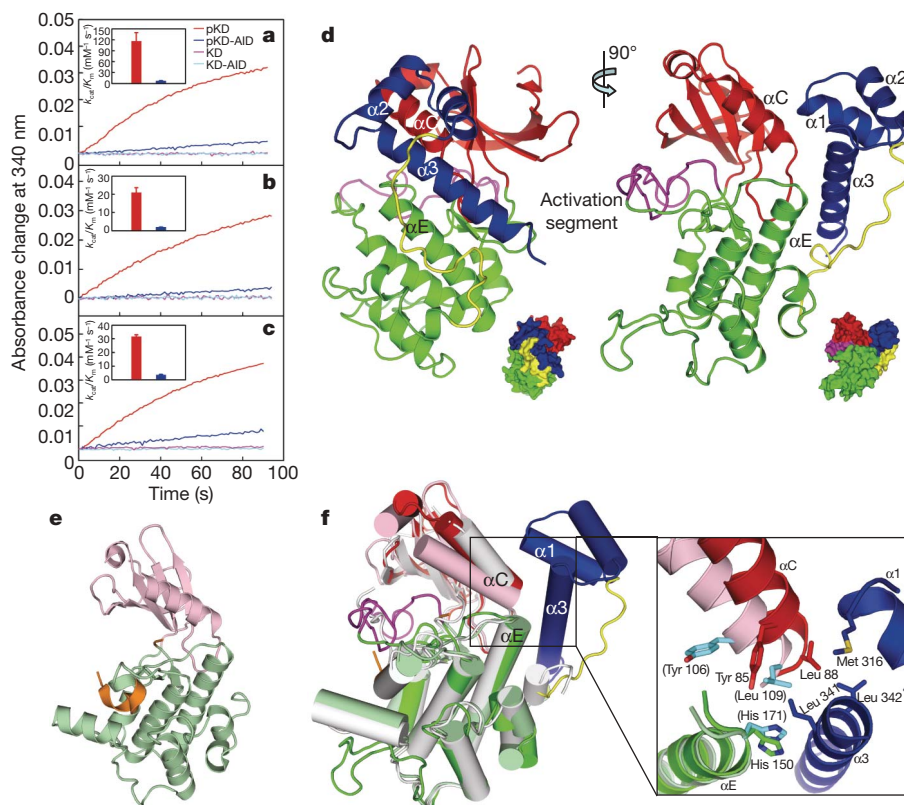


Figure 1 | Structure and activity of the AMPK kinase domain and KD-AID. **a–c**, Time courses of AMPK-catalysed SAMS (a modified peptide derived from residues 73–85 of rat acetyl-CoA carboxylase) phosphorylation. The absorption was recorded after the addition of 100 nM rat (a), 500 nM *S. pombe* (b), or 500 nM *S. cerevisiae* (c) AMPK proteins. The insets show the k_{cat}/K_m (SAMS) (Michaelis constant) values for phosphorylated proteins (mean and s.e.m., $n = 3$). **d**, Schematic and surface representations of *S. pombe* KD-AID in two views related by a 90° rotation around a vertical axis. The N- and C-lobes of the kinase domain are coloured in red and green, respectively, the activation segment is in magenta, the linker is in yellow, and the AID is in blue. **e**, Schematic representation of *S. cerevisiae* Snf1-pKD. The N- and C-lobes are coloured in light pink and pale green, respectively, and the activation segment is in orange. **f**, Superposition of the structures of *S. pombe* KD-AID, *S. cerevisiae* Snf1-pKD and Snf1-KD (PDB accession code 2FH9, in grey). In the close-up view on the right, corresponding KD-AID interface residues from Snf1-pKD are highlighted in cyan and labelled in parenthesis.

kinase domain and rat proteins. These data indicate that the dimers observed in our crystals are probably crystallization artefacts. The structural analyses hereafter were on the basis of monomer A of *S. cerevisiae* Snf1-pKD, and monomer B of *S. pombe* KD-AID, with lower average temperature factors (Supplementary Table 1).

Although no homologue structure was found for KD-AID in the PDB using the Dali server, the kinase domain and AID separately show high similarity to the kinase domain and ubiquitin-associated (UBA) domain of the AMPK-related protein kinases MARKs²⁴. Both the AID of AMPK and the UBA domain of MARK fold into a non-canonical UBA conformation, yet they differ in both their interaction mode and regulatory function (Fig. 2 and Supplementary Fig. 6). In MARK, the UBA domain binds exclusively to the N-lobe of its kinase domain, and is required for its phosphorylation^{24,25}. In contrast, the AID binds to the hinge region, opposite to the catalytic cleft of the kinase domain, and is not essential for the phosphorylation/activation of AMPK¹⁵ (Fig. 1). In KD-AID, both the N- and C-lobes of the kinase domain are engaged with the AID, resulting in the burial of ~1,500 Å² exposed surface area. The predominantly hydrophobic interactions mainly involve four helices: $\alpha 1$ and $\alpha 3$ from the AID and αC and αE from the kinase domain. In particular, the invariant Leu 341 on helix $\alpha 3$ penetrates into a groove lined by hydrophobic residues from both lobes of the kinase domain (Fig. 2c). In turn, highly conserved Leu 88 at the C terminus of helix αC nestles into a hydrophobic pocket on the AID, gated by Met 316 of helix $\alpha 1$ and Leu 342 of helix $\alpha 3$. As well as the hydrophobic contacts, the negatively charged Glu 344 on helix $\alpha 3$ of the AID interacts with positively charged Arg 149 from the C-lobe, which also hydrogen bonds to the linker connecting the AID with its kinase domain (Fig. 2d). The side chain of the next residue Asn 345 is in contact with Tyr 146 from the C-lobe and Arg 90 from the N-lobe. This interaction mode contrasts sharply with that observed in MARK, in which the UBA domain binds, mainly through its helix $\alpha 3$, onto the concave outer face of the N-lobe β -sheet of its kinase domain (Supplementary Fig. 6b). In view of the marked difference, the observed interaction mode between AMPK kinase domain and its AID is distinct from that in the predicted model for the human AMPK $\alpha 1$ -subunit fragment⁸.

Many kinases are regulated, in addition to phosphorylation on the activation segments, through protein–protein interactions involving their kinase domains^{22,23,26}. We wondered how AID-binding retains the kinase domain in a low-activity conformation. A close-up view of the superposition of kinase domains from *S. pombe* KD-AID and Snf1-pKD shows that residues from helix αC of a phosphorylated kinase domain could introduce a steric clash with the side chains of the key interface residues on the AID. For instance, owing to the inward and downward movement of helix αC , the ambulant side chain of Leu 109 in Snf1-pKD (Leu 88 in *S. pombe* KD-AID) may block the hydrophobic pocket for AID binding (Fig. 1f). Conversely, AID binding probably constrains the mobility of helix αC , resulting in a ‘relative open’ kinase conformation. Thus, this result discloses a unique mechanism for modulating kinase activity by directly interacting with helices αC and αE , although the interaction mode of AID binding to the backside of its kinase domain is reminiscent of the intramolecular autoinhibition mode observed in ZAP70 (ref. 27).

To assess the importance of the aforementioned interactions, we generated a series of point mutations on the *S. pombe* KD-AID fragment and examined their effect on catalytic function (Fig. 3a). When the key hydrophobic residues on the AID interface were individually replaced by charged residues (L341D, L342D and M316E), their catalytic efficiencies were increased approximately tenfold, comparable to that of the wild-type kinase domain. Mutant E344K, engineered to disrupt the hydrophilic interactions, yielded a modest but marked increase in basal activity, whereas substitution of the next residue (N345A) had little effect. To determine the role of the short linker connecting the AID to the kinase domain, we mutated Arg 280 that anchors the linker via four hydrogen bonds (Fig. 2c). The R280A mutation had no effect on kinase activity. However, mutating Leu 312 at the hydrophobic core of the AID to charged Asp (L312D) led to marked enzymatic activation (Supplementary Fig. 6d), which indicates that integrity of the AID is also required for its inhibitory function. We also mutated two crucial residues on the kinase domain interface, L88A and R149E, and these kinase-domain mutants had decreased catalytic activities. Nevertheless, the corresponding mutants in the background of KD-AID had similar kinase activities,

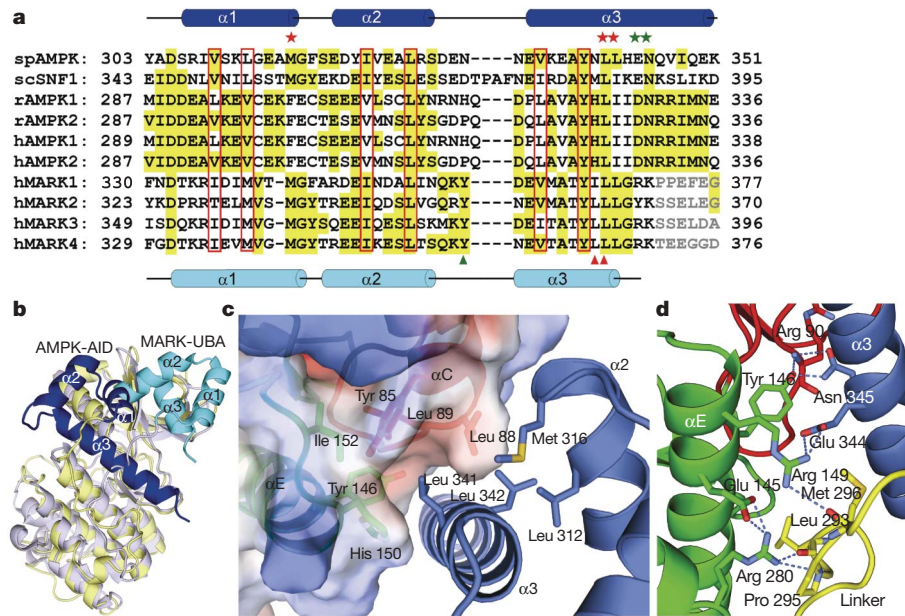


Figure 2 | The AID immobilizes the open conformation of kinase domain. **a**, Sequence alignment of AMPK-AIDs and MARK-UBAs. The hydrophobic core residues are boxed in red. Residues of AMPKs involving in hydrophobic and hydrophilic contacts with kinase domain are indicated by red and green asterisks, respectively, and those of MARKs by triangles. **b**, Structural comparison of *S. pombe* KD-AID with MARK1 KD-UBA (PDB accession code 2HAK). The kinase domain and the AID of AMPK are coloured in yellow and blue, respectively, and the kinase domain of MARK1 is in blue-white and the UBA domain is in cyan. **c**, van der Waals contacts at the KD-AID interface. The kinase domain is shown in surface representation, coloured according to electrostatic potential (positive, blue; negative, red). **d**, Hydrophilic interactions between the AID and the kinase domain.

indicating that these mutations also abolished AID inhibition (data not shown). These results indicate that the hydrophobic contacts between the kinase domain and the AID have a predominant role in controlling the conformational change between low- and high-activity forms of AMPK.

Because autoinhibition by the AID is universal to AMPK subfamily kinases, and as residues buried in the hydrophobic core of the AID are highly conserved (Figs 1 and 2), it is reasonable to postulate that rat

AMPK also has a functionally and structurally conserved autoinhibitory domain. We generated rat AMPK- $\alpha 1$ (also known as PRKAA1) mutants bearing mutations corresponding to those on the *S. pombe* KD-AID and examined their effects on kinase activity. As expected, in rat KD-AID mutants R263A and N330A there was little or no effect, whereas all others showed enhanced specific activities of more than 15-fold (Fig. 3b). To confirm the role of the AID further, we carried out a *trans*-inhibition assay using isolated rat AID, and the incomplete inhibition plateauing at $\sim 50\%$ provides evidence for the non-active-site binding of the AID (Fig. 3c and Supplementary Fig. 6e). Consistent with the effects of mutating the interface residues of the AID in *cis*-configuration, mutations in the isolated AID removed its *trans*-inhibition on the catalytic activity of kinase domain (Fig. 3c, inset).

As mammalian AMPK can be allosterically regulated by AMP binding to the γ -subunit, we next examined the effect of these mutations on the AMP activation of the rat AMPK holoenzyme. The wild-type heterotrimer is activated about twofold in the presence of 200 μM AMP, as reported⁷ (Supplementary Fig. 7a). Mutant N330A, with a slightly higher initial rate, retained a certain AMP-dependence, whereas the intrinsic activities of the remaining mutants were increased independently of AMP (Fig. 4a and Supplementary Fig. 7b). These data suggest that the AID is central to the allosteric control of AMPK by AMP. Therefore, we consider that the inhibition of AMPK kinase activity is probably due to the AID interaction but not the proposed pseudosubstrate contribution from the γ -subunit²⁸. Intriguingly, some of the mutants exhibited even higher activity than AMP-activated wild-type AMPK, which highlights the potential to develop new types of small compounds that activate AMPK by antagonizing the autoinhibition role of the AID, such as PT1 (ref. 29).

In addition to its allosteric effect, AMP was reported to markedly reduce the dephosphorylation rate of AMPK^{6,30}. Incubation of wild-type AMPK with human protein phosphatase 2C- α (PP2C- α , also known as PPM1A) alone led to marked dephosphorylation of pThr172, whereas the addition of AMP significantly slowed down the dephosphorylation rate (Fig. 4b and Supplementary Fig. 8). In contrast, the interface mutants drastically reduced the pThr172-dephosphorylation rate and largely abolished the AMP-dependence. These results indicate that the AID interaction may facilitate the dephosphorylation, and that this effect can be reversed by disruption of the KD-AID interface through mutation or by AMP-binding to the γ -subunit. Together, these mutagenesis data suggest a new conformational switch model for AMPK regulation: AMP binding to the

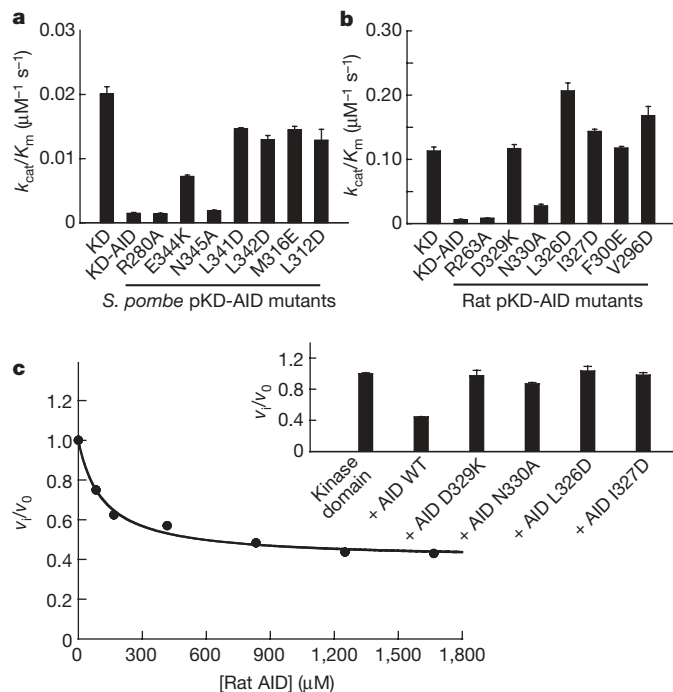


Figure 3 | Disruption of KD-AID interface abolishes AID inhibition.

a, b, Comparison of $k_{\text{cat}}/K_{\text{m(SAMS)}}$ values of KD-AID mutants (mean and s.e.m., $n = 3$). The assay was performed in the presence of 1 mM ATP, 10 μM SAMS and either 500 nM *S. pombe* (**a**) or 100 nM rat AMPK proteins. **c**, *Trans*-inhibition of the rat AID on the activity of its kinase domain. The assay was performed in the presence of 100 nM kinase domain, 20 μM SAMS, 1 mM ATP and various concentrations of the AID. The inset compares the inhibitory effects of wild-type AID and its mutants (mean and s.e.m., $n = 3$).

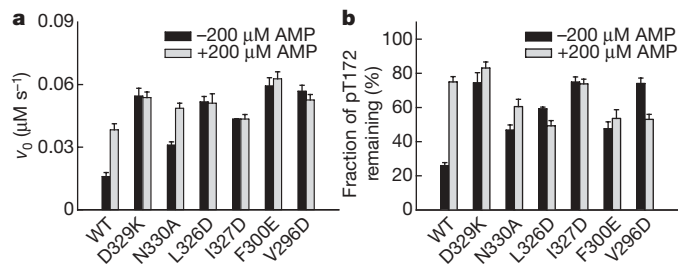


Figure 4 | Effect of KD-AID interface mutants on AMP-regulation of AMPK holoenzyme. a, Activity of AMPK heterotrimeric mutants independent of AMP change (mean and s.e.m., $n = 3$). The assay was performed in the presence of 2 nM AMPK, 1 mM ATP and 100 μM SAMs, with or without the addition of 200 μM AMP. **b**, Effects of mutations on AMP-protection of pThr 172 dephosphorylation (mean and s.e.m., $n = 3$). Phosphorylated AMPKs (7 μM) were treated with PP2C α (0.6 μM) for 40 min at 25 $^{\circ}\text{C}$, in the absence or presence of AMP (200 μM).

γ -subunit might transmit, by a yet unknown mechanism, onto the AID, alter the interaction between the AID and the kinase domain, and ultimately remove the effect of the AID on both kinase activation and pThr 172 dephosphorylation (Supplementary Fig. 9).

A long-standing paradox concerning the regulation of AMPK is that the α -subunit, in its isolated form, has little kinase activity and is apparently inhibited by the autoinhibitory sequence, and yet the AMPK holoenzyme is in a relatively active state⁷. To address this question, we further evaluated the role of the AID within heterotrimeric AMPK by detailed kinetic analyses. These analyses showed that the AID in the holoenzyme has a bona fide inhibiting role in the rate of phosphoryl transfer (catalytic constant, k_{cat}) as it does in the KD-AID, and that the catalytic activity and substrate binding affinity of AMPK are separately regulated by AMP binding and the assembly of β - and γ -subunits onto the α -subunit (Supplementary Table 2). Taken together, we have unravelled the structural basis of the autoinhibition of AMPK by the AID. The regulatory mode of AMPK by AMP provides a new mechanism by which autoinhibitory kinases are regulated by physiological signals.

METHODS SUMMARY

The kinase domain and KD-AID fragments of AMPKs from yeast and rat were subcloned and purified. The rat AMPK holoenzyme was expressed in a tricistronic vector. All mutants were generated by overlap PCR procedure. The purified proteins were stored at -80°C and glycerol was added to stocks used for enzymatic assay. Crystals of *S. pombe* KD-AID and *S. cerevisiae* Snf1-pKD were grown by mixing proteins with ammonium sulphate and ammonium formate, respectively. The structures were solved by molecular replacement and additional residues (of the AID fragment) were manually located. The data processing and refinement statistics are summarized in Supplementary Table 1. AMPK proteins were phosphorylated by CaMKK β , and the enzymatic activity of AMPK was determined by a coupled spectrophotometric assay. The kinetic parameters were obtained by fitting the experimental data to the Michaelis–Menten equation. The dephosphorylation of AMPK by PP2C α was analysed with western blotting.

Full Methods and any associated references are available in the online version of the paper at www.nature.com/nature.

Received 14 December 2008; accepted 17 April 2009.

Published online 27 May 2009.

- Carling, D. The AMP-activated protein kinase cascade—a unifying system for energy control. *Trends Biochem. Sci.* **29**, 18–24 (2004).
- Kahn, B. B., Alquier, T., Carling, D. & Hardie, D. G. AMP-activated protein kinase: ancient energy gauge provides clues to modern understanding of metabolism. *Cell Metab.* **1**, 15–25 (2005).
- Hardie, D. G. AMP-activated/Snf1 protein kinases: conserved guardians of cellular energy. *Nature Rev. Mol. Cell Biol.* **8**, 774–785 (2007).
- Hardie, D. G. AMP-activated protein kinase as a drug target. *Annu. Rev. Pharmacol. Toxicol.* **47**, 185–210 (2007).
- Yeh, L. A., Lee, K. H. & Kim, K. H. Regulation of rat liver acetyl-CoA carboxylase. Regulation of phosphorylation and inactivation of acetyl-CoA carboxylase by the adenylate energy charge. *J. Biol. Chem.* **255**, 2308–2314 (1980).

- Davies, S. P., Helps, N. R., Cohen, P. T. & Hardie, D. G. 5'-AMP inhibits dephosphorylation, as well as promoting phosphorylation, of the AMP-activated protein kinase. Studies using bacterially expressed human protein phosphatase-2C α and native bovine protein phosphatase-2A α . *FEBS Lett.* **377**, 421–425 (1995).
- Crute, B. E., Seefeld, K., Gamble, J., Kemp, B. E. & Witters, L. A. Functional domains of the α 1 catalytic subunit of the AMP-activated protein kinase. *J. Biol. Chem.* **273**, 35347–35354 (1998).
- Pang, T. et al. Conserved α -helix acts as autoinhibitory sequence in AMP-activated protein kinase α subunits. *J. Biol. Chem.* **282**, 495–506 (2007).
- Hawley, S. A. et al. Characterization of the AMP-activated protein kinase kinase from rat liver and identification of threonine 172 as the major site at which it phosphorylates AMP-activated protein kinase. *J. Biol. Chem.* **271**, 27879–27887 (1996).
- Scott, J. W. et al. CBS domains form energy-sensing modules whose binding of adenosine ligands is disrupted by disease mutations. *J. Clin. Invest.* **113**, 274–284 (2004).
- Iseli, T. J. et al. AMP-activated protein kinase β subunit tethers α and γ subunits via its C-terminal sequence (186–270). *J. Biol. Chem.* **280**, 13395–13400 (2005).
- McBride, A., Ghilagaber, S., Nikolaev, A. & Hardie, D. G. The glycogen-binding domain on the AMPK β subunit allows the kinase to act as a glycogen sensor. *Cell Metab.* **9**, 23–34 (2009).
- Cool, B. et al. Identification and characterization of a small molecule AMPK activator that treats key components of type 2 diabetes and the metabolic syndrome. *Cell Metab.* **3**, 403–416 (2006).
- Sanders, M. J. et al. Defining the mechanism of activation of AMP-activated protein kinase by the small molecule A-769662, a member of the thienopyridone family. *J. Biol. Chem.* **282**, 32539–32548 (2007).
- Göransson, O. et al. Mechanism of action of A-769662, a valuable tool for activation of AMP-activated protein kinase. *J. Biol. Chem.* **282**, 32549–32560 (2007).
- Scott, J. W. et al. Thienopyridone drugs are selective activators of AMP-activated protein kinase β 1-containing complexes. *Chem. Biol.* **15**, 1220–1230 (2008).
- Townley, R. & Shapiro, L. Crystal structures of the adenylate sensor from fission yeast AMP-activated protein kinase. *Science* **315**, 1726–1729 (2007).
- Amodeo, G. A., Rudolph, M. J. & Tong, L. Crystal structure of the heterotrimer core of *Saccharomyces cerevisiae* AMPK homologue Snf1. *Nature* **449**, 492–495 (2007).
- Xiao, B. et al. Structural basis for AMP binding to mammalian AMP-activated protein kinase. *Nature* **449**, 496–500 (2007).
- Rudolph, M. J., Amodeo, G. A., Bai, Y. & Tong, L. Crystal structure of the protein kinase domain of yeast AMP-activated protein kinase Snf1. *Biochem. Biophys. Res. Commun.* **337**, 1224–1228 (2005).
- Nayak, V. et al. Structure and dimerization of the kinase domain from yeast Snf1, a member of the Snf1/AMPK protein family. *Structure* **14**, 477–485 (2006).
- Nolen, B., Taylor, S. & Ghosh, G. Regulation of protein kinases: controlling activity through activation segment conformation. *Mol. Cell* **15**, 661–675 (2004).
- Pellicena, P. & Kuriyan, J. Protein–protein interactions in the allosteric regulation of protein kinases. *Curr. Opin. Struct. Biol.* **16**, 702–709 (2006).
- Marx, A. et al. Structural variations in the catalytic and ubiquitin-associated domains of microtubule-associated protein/microtubule affinity regulating kinase (MARK) 1 and MARK2. *J. Biol. Chem.* **281**, 27586–27599 (2006).
- Jaleel, M. et al. The ubiquitin-associated domain of AMPK-related kinases regulates conformation and LKB1-mediated phosphorylation and activation. *Biochem. J.* **394**, 545–555 (2006).
- Huse, M. & Kuriyan, J. The conformational plasticity of protein kinases. *Cell* **109**, 275–282 (2002).
- Deindl, S. et al. Structural basis for the inhibition of tyrosine kinase activity of ZAP-70. *Cell* **129**, 735–746 (2007).
- Scott, J. W., Ross, F. A., Liu, J. K. & Hardie, D. G. Regulation of AMP-activated protein kinase by a pseudosubstrate sequence on the gamma subunit. *EMBO J.* **26**, 806–815 (2007).
- Pang, T. et al. Small molecule antagonizes autoinhibition and activates AMP-activated protein kinase in cells. *J. Biol. Chem.* **283**, 16051–16060 (2008).
- Sanders, M. J. et al. Investigating the mechanism for AMP activation of the AMP-activated protein kinase cascade. *Biochem. J.* **403**, 139–148 (2007).

Supplementary Information is linked to the online version of the paper at www.nature.com/nature.

Acknowledgements We thank Y. Shi and S. C. Lin for critical discussions and reading of the manuscript; J. Chai and Y. Dong for help with data collection and processing; L. Gu and J. Wang for advice on structure determination. This work is supported in part by MOST grants 2006CB503900 and 2007CB914400, and by NSFC grants 30425005 and 30770476.

Author Contributions L.C., Z.-H.J. and L.-S.Z. designed, performed and analysed most of the experiments. Y.-Y.Z. and S.-T.X. provided technical assistance. Z.-X.W. contributed to discussions. J.-W.W. led the team and wrote the paper.

Author Information The structural and atomic coordinates have been deposited in the Protein Data Bank under accession codes 3H4J for *S. pombe* KD-AID and 3DAE for *S. cerevisiae* Snf1-pKD. Reprints and permissions information is available at www.nature.com/reprints. Correspondence and requests for materials should be addressed to J.W.W. (jjaweiwu@mail.tsinghua.edu.cn).

METHODS

Constructs, mutagenesis and protein purification. The KD-AID (residues 25–351) and kinase domain (25–297) of *S. pombe* AMPK α -subunit were amplified by standard PCR procedure from complementary DNA of strain SPQ-01 (provided by J. Liang) and inserted into pET28b vector by NcoI/XhoI sites with C-terminal His₆-tag. The KD-AID (residues 41–398) and kinase domain (41–315) of *S. cerevisiae* AMPK were amplified from genomic DNA of *S. cerevisiae* S288C (Invitrogen) and inserted into pET21b vector. The KD-AID (residues 1–358), kinase domain (1–280) and AID (284–358) of rat α 1-subunit (cDNA provided by P. Li) were also cloned into pET28b. The rat AMPK holoenzyme (α 1 β 1 γ 1) was expressed in a tricistronic vector as reported³¹. All mutants were generated by overlap PCR procedure and subjected to DNA sequencing. The expression vector of CaMKK β was provided by C. R. Mena. All proteins, overexpressed in *E. coli* BL21(DE3) cells at 20 °C, were first purified over Ni-NTA columns (Qiagen) and further polished by ion exchange and gel filtration chromatography (Source-15Q/15S and Superdex-200, GE Healthcare). The KD-AID fragments and kinase domains from *S. pombe*, *S. cerevisiae* and rat, phosphorylated or unphosphorylated, were stored at –80 °C and subjected to crystallization trials. Glycerol at a final concentration of 20% (v/v) was added into protein stocks used for enzymatic assay.

Crystallography. Crystals of *S. pombe* KD-AID were grown by the hanging-drop vapour diffusion method by mixing protein (~10 mg ml⁻¹) with an equal volume of reservoir solution containing 0.1 M sodium citrate, pH 5.6, 1.2 M ammonium sulphate. Crystals of *S. cerevisiae* Snf1-pKD were grown by mixing protein (~10 mg ml⁻¹) with an equal volume of reservoir solution containing 0.1 M Tris, pH 8.5, 4.0 M ammonium formate. Both crystals appeared after 2–3 days and grew to full size after 1 week. The crystals were cryoprotected in the reservoir solution supplemented with 20% glycerol and flash-frozen under cold nitrogen stream at 100K. The diffraction data set for KD-AID was collected at NW12 beam line at Photon Factory (Tsukuba, Japan) with an ADSC CCD detector, and that for Snf1-pKD collected at Beijing Synchrotron Radiation Facility with a CCD detector. Data were processed using HKL-2000 (ref. 32). The structures were solved by molecular replacement using Phaser³³ with one molecule from Snf1 kinase domain (PDB accession 3FAM) as search model²⁰. Additional residues that were not included in the search model were manually located. Standard refinement was performed with the programs Phenix³⁴ and Coot³⁵. The final model was refined to the *R* and *R*_{free} values of 21.8% and 25.7% for KD-AID and 22.7% and 26.6% for Snf1-pKD, respectively. The data processing and refinement statistics were summarized in Supplementary Table 1. All structural representations in this paper were prepared with Pymol (<http://www.pymol.org>).

Phosphorylation and activation of AMPK by CaMKK β . To determine the phosphorylation and activation time of AMPK by CaMKK β , the AMPK proteins were incubated in a phosphorylation buffer containing 50 mM Tris, pH 8.0, 2 mM DTT, 100 mM NaCl, 10 mM MgCl₂ and 1 mM ATP at 25 °C^{36,37}. The reactions were initiated by adding CaMKK β . Aliquots were withdrawn at indicated time intervals, and reactions were terminated by adding EDTA to a final concentration of 50 mM. The samples were then coupled to an AMPK kinase assay (see later) to directly examine the activation of AMPK by CaMKK β , and a maximum activation was observed after 30 min of incubation (Supplementary Fig. 2). The identical samples were also subjected to western blot analysis to examine the phosphorylation state using an antibody against the phospho-Thr 172 of AMPK (Cell

Signaling Technologies). In the following experiments, wild-type AMPK and all mutants (50 μ M) were preincubated in the phosphorylation buffer with CaMKK β (5 μ M) and ATP (1 mM) for 1 h before the kinase activity assay.

Kinetic analysis of kinase activity. The enzymatic activity of AMPK was determined, with SAMS peptide as substrate, using a coupled spectrophotometric assay^{38,39}. This assay couples the production of ADP with the oxidation of NADH by pyruvate kinase and lactate dehydrogenase (LDH). The standard assay was carried out at 25 °C in 1.8-ml reaction mixture containing 50 mM MOPS, pH 7.0, 100 mM NaCl, 0.1 mM EDTA, 10 mM MgCl₂, 0.2 mM NADH, 1.0 mM phospho(enol)pyruvate (PEP), 20 units ml⁻¹ LDH, and 15 units ml⁻¹ pyruvate kinase, and varying amounts of ATP, SAMS peptide and enzyme as indicated. Reactions were initiated by the addition of AMPK to the reaction mixture, and the enzymatic activity of AMPK was measured spectrophotometrically. Progress of the reaction was monitored continuously by following the formation of NAD⁺ at 340 nm, on a PerkinElmer Lambda 45 spectrophotometer equipped with a magnetic stirrer in the cuvette holder. Initial rates were determined from the linear slope of progress curves. The concentrations of ADP formed in AMPK-catalysed reaction were determined using an extinction coefficient for NADH of 6220 cm⁻¹ M⁻¹. The concentration of SAMS peptide was determined by turnover with the enzyme under conditions of limiting peptide at a fixed concentration of ATP. The kinetic parameters were obtained by fitting the experimental data to the Michaelis–Menten equation.

Dephosphorylation of AMPK by PP2C α . The phosphorylated wild-type AMPK and mutants (7 μ M) were incubated at 25 °C in a buffer containing 50 mM MOPS, pH 7.0, 100 mM NaCl, 0.1 mM EDTA and 2.5 mM MgCl₂, in the presence or absence of recombinant PP2C α (0.6 μ M) and AMP (200 μ M). At indicated time intervals, aliquots were removed from the reservoir and the reaction was terminated by the addition of gel-loading buffer. Samples were resolved by SDS–PAGE and subjected to western blot analysis using a phospho-specific anti-AMPK pThr 172 antibody.

- Neumann, D., Woods, A., Carling, D., Wallimann, T. & Schlattner, U. Mammalian AMP-activated protein kinase: functional, heterotrimeric complexes by co-expression of subunits in *Escherichia coli*. *Protein Expr. Purif.* **30**, 230–237 (2003).
- Otwinowski, Z. & Minor, W. Processing of X-ray diffraction data collected in oscillation mode. *Methods Enzymol.* **276**, 307–326 (1997).
- McCoy, A. J. et al. Phaser crystallographic software. *J. Appl. Crystallogr.* **40**, 658–674 (2007).
- Adams, P. D. et al. PHENIX: building new software for automated crystallographic structure determination. *Acta Crystallogr. D* **58**, 1948–1954 (2002).
- Emsley, P. & Cowtan, K. Coot: model-building tools for molecular graphics. *Acta Crystallogr. D* **60**, 2126–2132 (2004).
- Woods, A. et al. Identification of phosphorylation sites in AMP-activated protein kinase (AMPK) for upstream AMPK kinases and study of their roles by site-directed mutagenesis. *J. Biol. Chem.* **278**, 28434–28442 (2003).
- Hawley, S. A. et al. Calmodulin-dependent protein kinase kinase- β is an alternative upstream kinase for AMP-activated protein kinase. *Cell Metab.* **2**, 9–19 (2005).
- Roskoski, R. Jr. Assays of protein kinase. *Methods Enzymol.* **99**, 3–6 (1983).
- Davies, S. P., Carling, D. & Hardie, D. G. Tissue distribution of the AMP-activated protein kinase, and lack of activation by cyclic-AMP-dependent protein kinase, studied using a specific and sensitive protein assay. *Eur. J. Biochem.* **186**, 123–128 (1989).